Proc. Natl. Acad. Sci. USA
Vol. 84, pp. 4094–4098, June 1987
Biophysics

Evidence for the involvement of more than one metal cation in the Schiff base deprotonation process during the photocycle of bacteriorhodopsin

(Eu^{3+} concentration dependence/cation environments/cation participation/effect of photocycle/deprotonation mechanism)

TIMOTHY C. CORCORAN, KAMAL Z. ISMAIL*, AND MOSTAFA A. EL-SAYED†

Department of Chemistry and Biochemistry, University of California, Los Angeles, CA 90024

Contributed by Mostafa A. El-Sayed, December 8, 1986

ABSTRACT **The removal of metal cations inhibits the deprotonation process of the protonated Schiff base during the photocycle of bacteriorhodopsin. To understand the nature of the involvement of these cations, a spectroscopic and kinetic study was carried out on bacteriorhodopsin samples in which the native Ca^{2+} and Mg^{2+} were replaced by Eu^{3+}, a luminescent cation. The decay of Eu^{3+} emission in bacteriorhodopsin can be fitted to a minimum of three decay components, which are assigned to Eu^{3+} emission from three different sites. This is supported by the response of the decay components to the presence of ^2H_2O and to the changes in the Eu^{3+}/bR molar ratio. The number of water molecules coordinated to Eu^{3+} in each site is determined from the change in its emission lifetime when ^2H_2O replaces H_2O. Most of the emission originates from two "wet" sites of low crystal-field symmetry—e.g., surface sites. Protonated Schiff base deprotonation has no discernable effect on the emission decay of protein-bound Eu^{3+}, suggesting an indirect involvement of metal cations in the deprotonation process. Adding Eu^{3+} to deionized bacteriorhodopsin increases the emission intensity of each Eu^{3+} site linearly, but the extent of the deprotonation (and color) changes sigmoidally. This suggests that if only the emitting Eu^{3+} ions cause the deprotonation and bacteriorhodopsin color change, ions in more than one site must be involved—e.g., by inducing protein conformation changes. The latter could allow deprotonation by the interaction between the protonated Schiff base and a positive field of cations either on the surface or within the protein.**

Bacteriorhodopsin (bR) is the only protein found in the purple membrane of *Halobacterium halobium*, a light-harvesting bacterium. It contains a single chromophore molecule, retinal, covalently bound via a protonated Schiff base (PSB) linkage to the ε-amino group of a lysine residue in the protein (1, 2). Upon absorbing a photon, it undergoes a photochemical cycle (3) consisting of at least four intermediates on time scales varying from pico- to milliseconds:

$$bR_{570} \rightarrow K_{610} \rightarrow L_{550} \rightarrow M_{412} \rightarrow O_{640} \rightarrow bR_{570}.$$

During this photocycle, protons are pumped across the cell membrane to the outside, establishing an electrochemical proton gradient used by the organism for metabolic processes such as ATP synthesis (ref. 4 and refs. therein). Protons are ejected from the cell at a rate comparable to the formation of the M_{412} intermediate (5, 6). A good correlation has been found between the number of protons pumped and the amount of the slow-decaying form of M_{412} (7). This intermediate is the only one in which the Schiff base is unprotonated (8, 9). Consequently, many studies have inferred that the PSB deprotonation is closely associated with the proton pump mechanism (for review see ref. 6).

Recently, a very simple electrostatic model (the cation model) was proposed (10) to account for the strong coupling between (10–14), and thus the similar mechanism of deprotonation of, the PSB and an acid with a pK_a value of 8.6–10 [possibly tyrosine or an aspartic acid with a very high pK_a (15)] during the $L_{550} \rightarrow M_{412}$ step in the photocycle. In this cation model, it was hypothesized that the field of a positively charged species interacts with both of these acidic species during the $L_{550} \rightarrow M_{412}$ step in the photocycle at a rate that is determined by the protein conformation changes. The electrostatic repulsion between the positive field and the positively charged PSB and its attraction to the anionic conjugate base of the other acid would lead to a reduction in the pK_a values of both of these weak acids. The field could result from a positively charged amino acid, such as arginine, or possibly from Mg^{2+} or Ca^{2+} cations within or on the surface of the protein (10).

Atomic absorption shows that native (i.e., unmodified) bR contains Ca^{2+} and Mg^{2+} (16). However, when the purple membrane (λ_{max}, 570 nm) is acidified (1) or deionized on a cation exchange column (17) or treated by several other methods, it turns blue (λ_{max}, 608 nm) and divalent cations are missing (16). These different processes may all cause the same perturbation to the active site if the native purple membrane to blue transformation is represented by a proton–cation displacement equilibrium (18). The purple color is restored by adding cations (e.g., Mg^{2+}, Ca^{2+}, Na^+, K^+, Pb^{2+}, La^{3+}) (16, 17). This large color change indicates that the cations must have a direct or indirect interaction with the chromophore (16). Moreover, Schiff base deprotonation (5, 16, 18–20) and the UV transient absorbance attributed to tyrosine deprotonation (21) are all inhibited in both acidified and deionized bR. Transient absorption (22) and time-resolved Raman studies (18, 23) have shown that it is only the deprotonation step that is inhibited when cations are removed or excess H^+ is added. Therefore, it may be that these cations are the charged species that come in proximity to the PSB and the other weak acid. On the other hand, they could be indirectly involved. This could occur in one of two ways. The metal cations could be placed on the surface and their positive field (penetrating reasonable distances due to the low protein dielectric constant) interacts with the two weak acids during the deprotonation process. Another possible involvement could occur if the metal cations control the protein conformation change during the $L_{550} \rightarrow M_{412}$ transformation so as to assist in moving a positively charged amino acid or

The publication costs of this article were defrayed in part by page charge payment. This article must therefore be hereby marked "*advertisement*" in accordance with 18 U.S.C. §1734 solely to indicate this fact.

Abbreviations: bR, bacteriorhodopsin; PSB, protonated Schiff base.

*Present address: Department of Chemistry, University of Pittsburgh, Pittsburgh, PA 15260.
†To whom reprint requests should be addressed.

metal cation into the interaction sphere of the PSB and the other weak acid (21).

To fully understand the mechanism of deprotonation of the PSB, it is obvious that a better comprehension of the role of metal cations is necessary. To study the environment of the metal cations and their effect on the active site, Eu^{3+} is used as a probe. Eu^{3+} is a luminescent species that can isomorphously replace Ca^{2+} in proteins (24). Changes in site symmetry and environment strongly affect its emission lifetime (25); furthermore, the change in the observed lifetimes when ^2H_2O replaces H_2O can give a quantitative estimate of the number of water molecules coordinated to Eu^{3+} in each site (25, 26). We also study the changes in the kinetics of the Eu^{3+} emission (and thus, in their environments), if any takes place, during the photocycle as bR is transformed into M_{412}.

Comparing the population of Eu^{3+} bound to each site to the extent of deprotonation and color change while titrating deionized bR with Eu^{3+} could distinguish between a direct or indirect participation of the metal cations in these processes. It could reveal whether only one or more of the emitting cations are involved in the deprotonation and color change processes. More than one cation is found to describe the observed results. This is discussed in terms of their possible involvement in protein conformation changes.

MATERIALS AND METHODS

Materials. *H. halobium* was grown from master slants of the ET1001 strain generously provided by W. Stoeckenius (University of California, San Francisco). bR was purified by using a combination of methods (27, 28). Eu^{3+}-restored bR was prepared by deionizing native bR (12), adding $EuCl_3$ (Aldrich; 99.9%) solution with a micropipette, washing twice using centrifugation with Milli-Q 18MΩcm water (Millipore) or ^2H_2O (99.7%; Cambridge Isotope Laboratories, Woburn, MA) and then resuspending in the same solvent (pH 5.5–6). Eu^{3+}/bR ratios are expressed as mol of Eu^{3+} added to mol of deionized bR using ε_{608} = 60,000 (17). Unless otherwise stated, ratios were ≈2, which gave unaggregated suspensions. The final bR concentration was ≈20 μM. Except for M_{412} trapping, data were taken at 20 ± 2°C.

Atomic Emission. The maximum number of Eu^{3+} that strongly bind to bR was determined by atomic emission spectrophotometry. A SPECTRAA 30 atomic absorption and emission spectrophotometer (Varian Techtron, Springvale, Australia) was used with an acetylene/nitrous oxide flame. These samples were prepared using a large excess of $EuCl_3$ and then washed repeatedly to eliminate unbound Eu^{3+}.

Emission Spectra. The doubled output of a Nd:YAG-pumped dye laser (Quanta-Ray, Mountain View, CA) at 280 nm was used to excite the tyrosine and tryptophan residues of the protein, which efficiently transferred energy to the Eu^{3+} bound to the protein. Spectra were recorded with a 1-m monochromator (Jarrell-Ash) using a 1-cm cuvette and a 90° collection angle. A $NaNO_2$ solution filter and a gated photomultiplier tube (switched off for 2 μs bracketing the laser pulse) (29) rejected the scattered laser light. A Model 162 boxcar averager (PAR, Princeton, NJ) selected the emission between 20 and 80 μs after the laser pulse. These samples were prepared in the same way as the atomic emission samples but were suspended in 50% (vol/vol) glycerol/water to cut down aggregation.

Excitation Spectra. Excitation spectra were taken using the above apparatus, but substituting a combination of long- and short-pass filters for the monochromator to select emission from the $^5D_0 \rightarrow {}^7F_2$ band while scanning the $^5D_0 \leftarrow {}^7F_0$ transition. An f/0.5 concave spherical mirror was used to collect the emission. The spectra were corrected for laser intensity changes with wavelength.

Emission Lifetimes. Emission lifetimes were taken with the same detection apparatus as the excitation spectra, but a nitrogen-pumped dye laser (PRA International, London, ON, Canada, LN1000 and LN102) at 393 nm (120 μJ, 0.5-ns pulse, 9-Hz repetition rate) excited the much stronger Eu^{3+} $^5L_6 \leftarrow {}^7F_0$ absorbance, and emission from the $^5D_0 \rightarrow {}^7F_2$ transition was collected off the front surface of a 2-mm cuvette to minimize inner filter effects. A transient digitizer (Biomation 805, Gould Electronics, Santa Clara, CA) and a signal averaging computer (Apple II+) were used to record the data. Between 2048 and 8192 shots were averaged. We corrected for the small amount of detected laser scatter by subtracting a background using Eu^{3+}-free bR. Analysis was performed on a VAX 11-780 minicomputer using a Marquardt method nonlinear least-squares fitting program (30). The first 10 μs after the laser flash were not fit to allow complete recovery of the gated photomultiplier tube.

M_{412} Trapping. For M_{412} trapping, sealed cuvettes were immersed in a quartz dewar filled with methanol cooled by addition of liquid N_2 to −40 ± 4°C, since the M_{412} decay is very slow at this temperature (31). The Eu^{3+}-restored bR was suspended in 66% (vol/vol) glycerol/water to avoid freezing. The glycerol (Aldrich; spectrophotometric grade) was photooxidized to remove trace luminescent contaminants. The sample was illuminated with a 500-W tungsten projector lamp through a 570-nm narrow-band (10-nm) interference filter. This light was focused to a spot roughly 10 mm in diameter and was incident at an angle of ≈20° to the ≈6-mm diameter excitation laser. Care was taken to ensure good overlap of the two beams. The tungsten lamp was chopped to eliminate scattering during the emission lifetime measurements, which were made as described above.

RESULTS

Emission and Excitation Spectra of Eu^{3+} in bR. The emission spectra of $EuCl_3$ (≈75 mM in H_2O) and Eu^{3+}-restored bR are shown in Fig. 1. It is clear that the transitions from the $^5D_0$ level to the $^7F_2$ levels have become much more radiatively

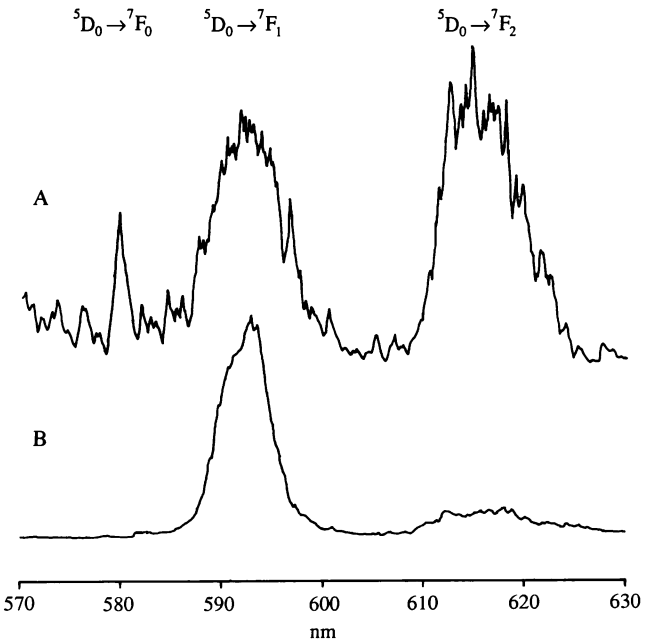

FIG. 1. Emission spectra of Eu^{3+} bound to bR (*A*) and in aqueous solution (*B*). Note the presence of the $^5D_0 \rightarrow {}^7F_0$ band and the higher intensity of the $^5D_0 \rightarrow {}^7F_2$ transition in bR as compared to that in water, which strongly suggests that the symmetry has been greatly reduced when the ion is bound to the protein.

allowed (relative to the $^7F_1$ level) in the protein compared to the corresponding transitions in aqueous solution. This strongly suggests that the crystal field symmetry around the protein-bound Eu^{3+} is greatly reduced from that found in aqueous Eu^{3+} [which is D_{2h} (32)] and has lost its center of symmetry. This is to be expected if each Eu^{3+} is coordinated to a low-symmetry arrangement (24) of H_2O and COO- (33) groups in the protein, which induce the dominant portion of the crystal field. Similar changes in Eu^{3+} absorption spectra and radiative rates upon changes of chelates and solvents have been reported (25, 32, 34).

Excitation spectra were taken to determine whether Eu^{3+} occupying different sites within the protein are spectrally resolvable, since it has been shown that for the narrow $^5D_0 \leftarrow {}^7F_0$ transition changes in chelation can cause clearly resolved shifts in this band (26). However, only a single, unchanging band was seen for Eu^{3+}-restored bR ranging from one to three Eu^{3+} per bR (data not shown). A much more sensitive method to detect different sites is to examine the Eu^{3+} emission decays.

Eu^{3+} Emission Decays. *Minimum number of sites.* We have found that the observed decays required a sum of a minimum of three exponentials to be fit adequately using nonlinear least squares. Biexponential fits were clearly inadequate (Fig. 2), and a sum of four exponentials did not reveal another well-separated component. The lifetimes each differ by factors of 4 or more from the next component, making the triexponential fit possible.

We examined well-washed samples restored with an excess of Eu^{3+} by flame atomic emission spectrophotometry and found they contained $\approx$4 Eu^{3+} per bR molecule. This together with other experimental results suggest that deionized bR can strongly bind two to four metal cations (16–18, 35, 36). It is thus tempting to assign the three components of the Eu^{3+} decay to different distinguishable sites for Eu^{3+} binding. If so, then it is also possible that a certain decay component (e.g., the shortest) could correspond to two bound Eu^{3+} per bR. This gives us a microscopic probe, allowing us to independently examine the response of different emitting Eu^{3+} sites to different perturbations.

The values of the lifetimes and relative amplitudes are given in Table 1. The major components of Eu^{3+} in bR (32 μs and 230 μs) are much faster than the 3- to 4-ms lifetime observed for $EuCl_3$ in ^2H_2O, which has a quantum yield not far from unity (37). This together with our observation that

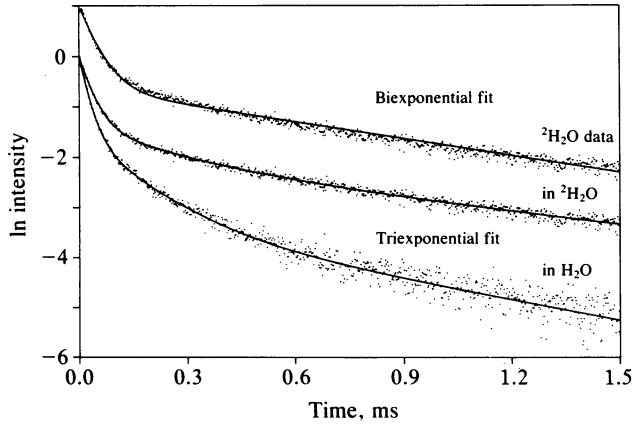

FIG. 2. Eu^{3+} emission decays in bR. Logarithmic plots are used to show the multiexponential behavior. Dots represent individual data points; solid lines are the fitted curves. Eu^{3+} emission decay in bR suspended in H_2O and ^2H_2O fitted to a sum of three exponentials. From the change in the observed rates, the number of water molecules coordinated with each Eu^{3+} in the different sites can be calculated (see Table 1). A biexponential fit to the ^2H_2O data is shown (upper trace) for comparison. This fit is clearly inadequate.

the transitions to both the $^7F_2$ and $^7F_0$ levels have strong emission intensity might suggest that the decrease in the observed lifetimes is a result of a large increase in the radiative probability. This implies a large reduction in the crystal field symmetry of Eu^{3+} in these sites compared to those in water.

Concentration dependence. Emission decays were measured as a function of Eu^{3+}/bR ranging from 1 to 3. Neither the relative amplitudes nor the lifetimes of the emission from the different sites varied significantly as the Eu^{3+}/bR ratio increased. This implies that the fraction of Eu^{3+} bound to each of the different sites did not vary in this range. Meanwhile, the total emission intensities immediately after the laser flash were found to increase linearly with the Eu^{3+}/bR ratio. Fig. 3 (*Upper*) depicts the combination of these two types of results. It shows that the total intensity from all the emitting sites and that from each individual site increases linearly with the Eu^{3+} concentration.

Cation environments. Eu^{3+} emission lifetimes were recorded in H_2O and ^2H_2O (Fig. 2). The difference in the observed luminescence rates, $\Delta\tau^{-1}$, has been demonstrated by Horrocks and Sudnick (26) to be directly proportional to the number of coordinated water molecules. Following their method, we calculate the number of coordinated H_2O molecules from $\Delta\tau^{-1}$. The results (Table 1) indicate that the Eu^{3+} site corresponding to the fastest component is quite wet, interacting with >6 H_2O molecules. It is probably a very low symmetry site on the surface of the protein. The site corresponding to the second component is moderately wet, with $\approx$3 H_2O molecules. The site corresponding to the third component (giving rise to a minor portion of the Eu^{3+} emission intensity) is probably in a hydrophobic region.

Effect of M_{412} formation on the Eu^{3+} environment. We examined the emission lifetime of Eu^{3+}-restored bR suspended in glycerol/water at −40°C. If bR is exposed to strong excitation at 570 nm at this temperature, a large steady-state population of the M_{412} intermediate is formed (31). Under these conditions, we found that >50% of the sample was in the M_{412} intermediate at pH $\approx$6. The decay kinetics for this sample are compared with those for the same sample without M_{412} trapping in Table 1. Within experimental error, it seems that driving the cycle to form M_{412}‡ does not perturb the luminescent sites of Eu^{3+}. Transient absorbance measurements show that the laser pulse at this wavelength and intensity does not cause substantial pumping of the photocycle or depletion of trapped M_{412} population.

DISCUSSION

The main results can be summarized as follows:

(*i*) Flame atomic emission shows four Eu^{3+} are bound when excess Eu^{3+} is added to bR and then washed repeatedly. This implies that there are up to four distinct Eu^{3+} binding sites in bR, in agreement with the work of Ariki and Lanyi (35) and Katre *et al.* (36).

(*ii*) From the laser-excited emission decays, three different components are observed for Eu^{3+} bound to bR in the range of 1–3 Eu^{3+} per bR. These different decay components are assigned to Eu^{3+} in three different sites (environments). This assignment is supported by the presence of up to four strongly bound Eu^{3+} per bR (refs. 16–18, 35, and 36, and our flame atomic emission results); the variation in the lifetimes of these three components in ^2H_2O compared to H_2O; and the increase in the intensity of each site as the Eu^{3+} concentration added to blue bR increases.

‡One must be cautious, however, since there may be some differences between the form of M_{412} found at room temperature and that found at −40°C by trapping.

Table 1. Triexponential Eu^{3+} emission kinetics (lifetimes and normalized amplitudes)* in H_2O and ^2H_2O and the water coordination numbers of the emitting sites in bR and the effect of trapping the M_{412} intermediate

Component number	Lifetime, ms (amplitude)		$\Delta\tau^{-1}$, ms^-	Coordination number
	In H_2O†	In ^2H_2O†		
1	0.025 ± 0.001 (0.78)	0.032 ± 0.003 (0.69)	9.0 ± 3.3	6–9
2	0.14 ± 0.01 (0.18)	0.23 ± 0.05 (0.17)	2.9 ± 1.1	2–4
3	0.70 ± 0.04 (0.04)	1.2 ± 0.1 (0.14)	0.6 ± 0.1	≈0.5
	With ≈50% M_{412}‡	No M_{412}‡		
1	0.04 ± 0.02 (0.53 ± 0.06)	0.036 ± 0.006 (0.49 ± 0.08)		
2	0.25 ± 0.04 (0.42 ± 0.07)	0.24 ± 0.02 (0.45 ± 0.06)		
3	0.9 ± 0.2 (0.06 ± 0.01)	1.0 ± 0.2 (0.06 ± 0.02)		

*Uncertainties given are standard deviations.
†At 20 ± 2°C.
‡At −40 ± 4°C in 66% glycerol/H_2O.

(*iii*) The observation of three components, when the flame atomic emission data indicate four sites, could either suggest that two of the Eu^{3+} sites have similar decay constants (i.e., similar environments) or else the fourth site completely quenches the luminescence—e.g., if the Eu^{3+} is very near the retinal.

(*iv*) Two sites give rise to the majority of the Eu^{3+} luminescence intensity. The Eu^{3+} in these sites have relatively short lifetimes and are coordinated to water. This together with the fact that the emission spectrum suggests very low crystal-field symmetry and large radiative probability for this presumably forbidden transition strongly suggests that most of the emitting Eu^{3+} are located on or near the surface in a hydrophilic environment. The Eu^{3+} that gives rise to a minor portion of the luminescence intensity has a long lifetime and is located in a hydrophobic environment.

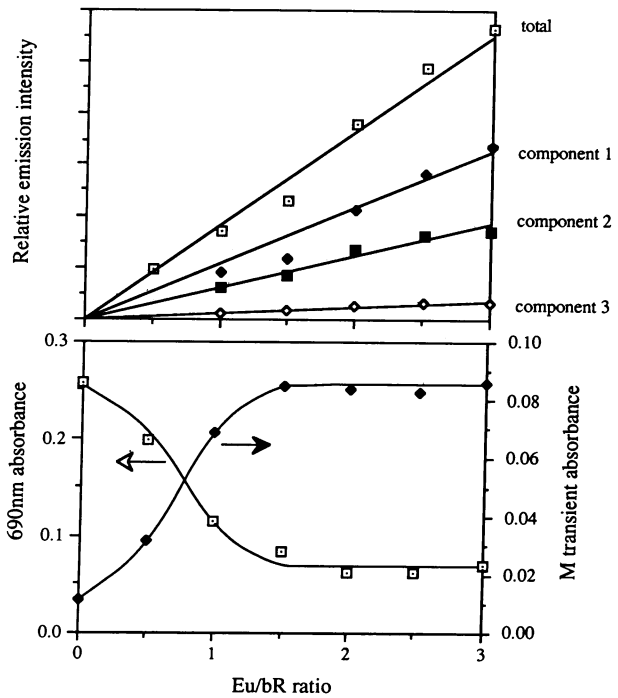

FIG. 3. Comparison between the effect of adding Eu^{3+} to deionized bR on the total emission intensity and that of the individual components (i.e., sites) (*Upper*) and the extent of retinal color change and Schiff base deprotonation (*Lower*). The latter results are similar to those observed previously when deionized bR is regenerated by adding either Eu^{3+} (35) or Ca^{2+} (18). (See ref. 18 for experimental details.) The fact that the concentration of Eu^{3+} in the different sites increases linearly while their effect on the Schiff base deprotonation (i.e., M_{412} formation) and the retinal color change varies sigmoidally with the Eu^{3+}/bR ratio suggests more than one metal cation is involved in the latter processes.

(*v*) From the observed linear dependence of the Eu^{3+} emission intensity of each and all the sites on the Eu^{3+} concentration, it is concluded that the binding constants are comparable for the different emitting Eu^{3+} sites. This is contrary to previous conclusions (35, 36). Katre *et al.* observed a large increase (from one to three) in the number of cation sites in their (*n*)Pb^{2+} − $3Ca^{2+}$ Fourier difference x-ray diffraction patterns (36) in bR as the Pb^{2+}/bR ratio increases from 1 to 2. However, their observation could in fact be due to changes in the protein conformation (17).

(*vi*) In agreement with previous results, the bottom of Fig. 3 shows that both the chromophore color (16–18, 35) and the amount of M formation (18, 35) change with a sigmoidal dependence on the amount of cations added to deionized bR. This, combined with the conclusion reached in *v* above, might suggest that the change in the retinal color as well as the deprotonation process are not due to the interaction of the retinal system with any individual metal cation but rather requires more than one metal cation in different sites.§ As the metal cations occupy different sites, they could cause a protein conformational change around the active site when a required minimum of charges are bound to more than one site. A change in the protein conformation upon adding metal cations to deionized bR was previously concluded from the observed changes in the protein CD spectrum (17). In this protein conformation, the penetrating field of the surface metal cations could lead to the color change of the retinal and/or the deprotonation of the PSB during the photocycle. On the other hand, this protein conformation could place a positively charged amino acid (or the "fourth" nonemitting Eu^{3+} if present) near the PSB during the $L_{550} \rightarrow M_{412}$ transformation, thus leading to deprotonation.

(*vii*) The conclusion that the interaction with the emitting Eu^{3+} is indirect can be further supported by the observation that the formation of M_{412} does not change the environment of any of the individual emitting Eu^{3+} sites. This suggests that the deprotonation process does not involve any of the emitting Eu^{3+} at near interaction distances. If surface charges control the conformation of the protein around the active site, which in turn controls the retinal color and the deprotonation of the PSB during the cycle, one may propose that the native purple form, the deionized blue membrane, and the blue and purple forms of bR found at low pH (1, 19) represent different protein conformations stable at different amounts of surface charges (i.e., different amounts of H^+, metal cations, organic cations, or anions).

§A simple model shows (38) that the two sites can indeed give a sigmoidal type behavior for equal binding constants.

M.A.E. would like to thank Prof. W. Stoeckenius for a number of fruitful discussions. The advice of Prof. R. Bogomolni and Ms. Kathleen McGuinness (all of the University of California, San Francisco) on the growth and purification of bR is greatly appreciated. This work was supported by a grant from the Department of Energy (Office of Basic Energy Sciences).

1. Oesterhelt, D. & Stoeckenius, W. (1971) *Nature (London) New Biol.* **223,** 149–152.
2. Bridgen, J. & Walker, I. D. (1976) *Biochemistry* **15,** 792–798.
3. Lozier, R., Bogomolni, R. A. & Stoeckenius, W. (1975) *Biophys. J.* **15,** 955–962.
4. Bogomolni, R. A., Baker, R. A., Lozier, R. H. & Stoeckenius, W. (1976) *Biochim. Biophys. Acta* **440,** 68–88.
5. Drachev, L. A., Kaulen, A. D. & Skulachev, V. P. (1978) *FEBS Lett.* **87,** 161–167.
6. Ottolenghi, M. (1980) *Adv. Photochem.* **12,** 97–200.
7. Li, Q.-Q., Govindjee, R. & Ebrey, T. G. (1984) *Proc. Natl. Acad. Sci. USA* **81,** 7079–7082.
8. Lewis, A., Spoonhower, J., Bogomolni, R. A., Lozier, R. H. & Stoeckenius, W. (1974) *Proc. Natl. Acad. Sci. USA* **71,** 4462–4466.
9. Aton, B., Doukas, A., Callender, R. H., Becher, B. & Ebrey, T. G. (1977) *Biochemistry* **16,** 2995–2999.
10. Hanamoto, J. H., Dupuis, P. & El-Sayed, M. A. (1984) *Proc. Natl. Acad. Sci. USA* **81,** 7083–7087.
11. Hess, B. & Kuschmitz, D. (1979) *FEBS Lett.* **100,** 334–340.
12. Corcoran, T. C., Dupuis, P. & El-Sayed, M. A. (1986) *Photochem. Photobiol.* **43,** 655–660.
13. Scherrer, P., Packer, L. & Seltzer, S. (1981) *Arch. Biochem. Biophys.* **212,** 589–601.
14. Scherrer, P. & Stoeckenius, W. (1984) *Biochemistry* **23,** 6195–6202.
15. Engelhard, M., Gewert, K., Hess, B., Kreutz, W. & Siebert, F. (1985) *Biochemistry* **24,** 400–407.
16. Chang, C.-H., Chen, J.-G., Govindjee, R. & Ebrey, T. (1985) *Proc. Natl. Acad. Sci. USA* **82,** 396–400.
17. Kimura, Y., Ikegami, A. & Stoeckenius, W. (1984) *Photochem. Photobiol.* **40,** 641–646.
18. Chronister, E. L., Corcoran, T. C., Song, L. & El-Sayed, M. A. (1986) *Proc. Natl. Acad. Sci. USA* **83,** 8580–8584.
19. Mowery, P. C., Lozier, R. H., Chase, Q., Tseng, Y.-W., Taylor, M. & Stoeckenius, W. (1979) *Biochemistry* **18,** 4100–4107.
20. Chang, C.-H., Suh, C.-K., Govindjee, R. & Ebrey, T. (1984) *Biophys. J.* **45,** 210a (abstr.).
21. Dupuis, P., Corcoran, T. C. & El-Sayed, M. A. (1985) *Proc. Natl. Acad. Sci. USA* **82,** 3662–3664.
22. Ohtani, H., Kobayashi, T., Iwai, J. & Ikegami, A. (1986) *Biochemistry* **25,** 3356–3363.
23. Chronister, E. L. & El-Sayed, M. A. (1987) *Photochem. Photobiol.* **45,** 507–513.
24. Matthews, B. W. & Weaver, L. H. (1974) *Biochemistry* **13,** 1719–1725.
25. Kropp, J. L. & Windsor, M. W. (1965) *J. Chem. Phys.* **42,** 1599–1608.
26. Horrocks, W. DeW., Jr., & Sudnick, D. R. (1981) *Acc. Chem. Res.* **14,** 384–392.
27. Oesterhelt, D. & Stoeckenius, W. (1974) *Methods Enzymol.* **31,** 667–678.
28. Becher, B. M. & Cassim, J. Y. (1975) *Prep. Biochem.* **5,** 161–178.
29. Hopewell, W. D. (1980) Dissertation (Univ. of California, Los Angeles), pp. 36–42.
30. Bevington, P. R. (1967) *Data Reduction for the Physical Sciences* (McGraw-Hill, New York), pp. 237–240.
31. Chance, B., Porte, M., Hess, B. & Oesterhelt, D. (1975) *Biophys. J.* **15,** 913–917.
32. Sayre, E. V., Miller, D. G. & Freed, S. (1957) *J. Chem. Phys.* **26,** 109–113.
33. Chang, C.-H., Jonas, R., Melchiore, S., Govindjee, R. & Ebrey, T. (1986) *Biophys. J.* **49,** 731–739.
34. Miller, D. G., Sayre, E. V. & Freed, S. (1958) *J. Chem. Phys.* **29,** 454–455.
35. Ariki, M. & Lanyi, J. K. (1986) *J. Biol. Chem.* **261,** 8167–8174.
36. Katre, N. V., Kimura, Y. & Stroud, R. M. (1986) *Biophys. J.* **50,** 277–284.
37. Stein, G. & Wurzberg, E. (1974) *J. Chem. Phys.* **62,** 208–213.
38. Corcoran, T. C., Awad, E. S. & El-Sayed, M. A. (1987) *Proceedings of the 12th Taniguchi Symposium on Primary Processes in Photobiology* (Springer, Berlin), in press.